KEK Preprint 96-23
DPNU 96-28
KUDP 96/01
TUAT-HEP 96-2
H

Measurements and Calculations of Gravitational and Electrostatic Wire Sags for a 4.6 Meter Long Drift Chamber

S.Sudou[a], *N.Khalatyan*[b], *Y.Kurihara*[b], *T.Abe*[c], *K.Fujii*[b], *A.Sugiyama*[c], *K.Takahashi*[a], *T.Watanabe*[d]

[a]Tokyo University of Agriculture and Technology, Tokyo 184
[b]KEK, National Laboratory for High Energy Physics, Tsukuba 305, Japan
[c]Department of Physics, Nagoya University, Nagoya 464, Japan
[d]Kogakuin University, Tokyo 163-91, Japan

Abstract

Measurements of wire tensions, gravitational and electrostatic sags for a 4.6m test chamber are described. A method to calculate the wire sags knowing the initial position of and tension and high voltage on each wire is developed. There is a good agreement between measurement and calculation.

1 Introduction

One of the most important goals of experiments at a future linear e^+e^- collider such as JLC[1] is to discover and study the Higgs boson. In particular, if one wants to confirm the narrowness of the Higgs boson by measuring the distribution of the recoil mass opposite to the lepton pair from the Z^0 boson decay in the process $e^+e^- \to H^0Z^0$, the recoil mass resolution should at least be as good as the beam energy spread of the collider. This requires a high resolution central tracker with a momentum resolution of $\sigma_{p_T}/p_T \sim 10^{-4} \times p_T(\text{GeV})$. Such a tracking chamber becomes as large as 2.3 m in radius, even if we assume 100 sampling points with a spatial resolution of 100μm per wire in a magnetic field of as high as 2 T. In addition, to ensure this momentum resolution over a polar angle range of $45° < \theta < 135°$, the chamber has to be as long as 4.6 m. Due to substantial gravitational and electrostatic sags, achieving a spatial resolution of 100 μm/wire for a 4.6 m long chamber is quite non-trivial. We need to be able to predict wire positions very precisely under the influence of gravitational and electrostatic forces.

We have been developing a software program to predict wire displacement, knowing the cell structure, wire tension, and high voltage on each wire. The validity of the prediction has to be proved experimentally. We have developed a wire tension and position measurement system and measured wire tensions, gravitational and electrostatic sags for a 4.6 m long test chamber (see Fig. 1). The results of the measurements were then compared with the predictions.


Figure 1: 4.6 m CDC test chamber with wire position measurement system.

In this paper, we describe the method of wire sag calculations and measurements of gravitational and electrostatic wire sags using a newly developed wire position measurement system, and compare the calculations with the measurements so as to study feasibility of a high resolution drift chamber in the presence of significant wire sags. The paper is organized as follows. In section 2 we describe our test chamber parameters from a design philosophy point of view. Section 3 formulates the method of wire sag calculations in such a way that it is applicable to any wire configuration. The basic formulae derived there will clarify key quantities to be measured in order to test the validity of the method. The following two sections (4 and 5) are devoted to measurements of the key quantities, namely, wire tensions and gravitational and electrostatic wire sags. These measurements are then compared with the predictions in section 6. Finally section 7 summarizes our results and concludes this paper.

2 Test Chamber Parameters

In order to fulfill the physics requirements, we need to achieve the following performance goals:

- $\sigma_{r\phi} \simeq 100\ \mu$m
- $\sigma_{rz} \simeq 1$ mm
- two track separation better than 2 mm

in a magnetic field of 2 T for a wire length of 4.6 m. The second and the third of the above goals are to ensure good track-cluster matching in a jetty environment. One possible approach to realizing these design goals is to use a slow gas mixture with a small Lorentz angle and a mini-jet cell structure to allow stereo wires for z-coordinate measurements. We designed such a mini-jet cell so as to realize the design goals ignoring possible wire sag effects, since the electric field can be calculated to a good approximation in this way, if all the wires have the same gravitational sags.[2]

A possible cell design is shown in Fig. 2-(a) which also specifies our wire naming convention to be used hereafter. The cell has 5 sense wires ($S1$ to $S5$) held at 2.5 kV and

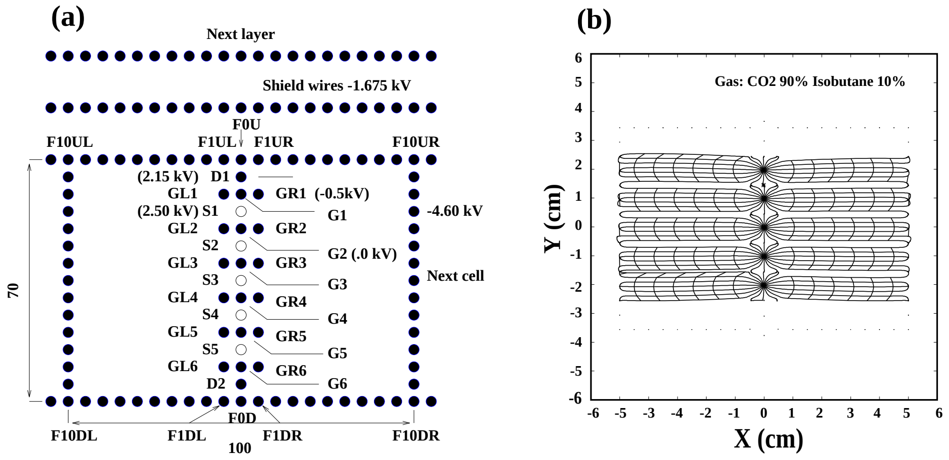

Figure 2: (a) possible mini-jet cell structure and (b) corresponding drift lines.

spaced 1 cm, with each surrounded by ground wires ($G1$ to $G6$) in the sense wire plane and grid wires ($GL1$ to $GL6$ and $GR1$ to $GR6$) at -0.5 kV placed 5 mm away from it. The two dummy sense wires ($D1$ and $D2$) at the both ends of the sense wire plane are held at 2.15 kV and stabilize the upper- and the lower-most sense wires ($S1$ and $S5$). The maximum drift length is 5 cm where the drift field is produced by 10 field shaping wires ($F1{*}{*}$ to $F10{*}{*}$) whose potentials change linearly in this order from -0.5 kV to -4.6 kV, and by left and right edge field wires held at -4.6 kV. The wire diameter is 30 μm for sense wires and 125 μm for the others. The high voltages on the wires were chosen so as to get as uniform a drift field as possible with minimum electrostatic forces, while keeping a reasonable gas gain for a chamber gas mixture of 90%CO_2 and 10% Isobutane. Fig. 2-(b) plots the drift lines calculated with a drift chamber simulation program GARFIELD [3].

Our 4.6 m long test chamber has seven identical cells with the cell parameters described above. The layout of the seven cells is shown in Fig. 3. Unless otherwise stated,

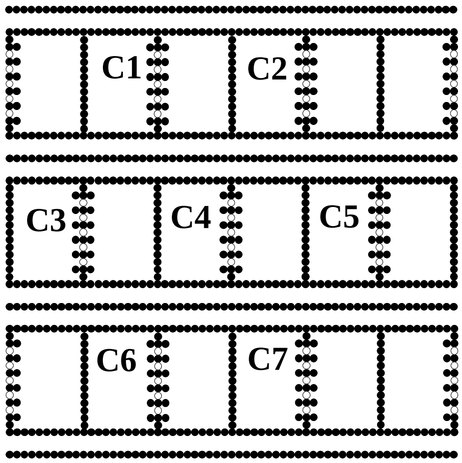

Figure 3: Cell layout of our 4.6 m long test chamber.

wires we are going to deal with belong to the central cell ($C4$).

Before stringing wires, we surveyed the endplates to check their machining precision and found that the standard deviation of the actual wire hole positions from the nominal ones to be less than 8.2 μm. The sense wires are gold-plated tungsten and all the other wires are gold-plated aluminum. The reason for this choice of Al as the wire material is to minimize the total wire tension so as to reduce the thickness of the chamber endplates as required by endcap calorimeters. The wire stringing took us three weeks.

3 Basic Formulae for Wire Sags

Wires in a drift chamber are subject to gravitational and electrostatic forces to be balanced by restoring forces from wire tension. The equation for the equilibrium position of a wire can be written in the form:

$$T \cdot \frac{d^2\vec{\delta}}{dz^2} = \vec{F}_e + \vec{F}_g, \tag{1}$$

where T is the wire tension, $\vec{\delta}(z) = \vec{\delta}_g + \vec{\delta}_e$ is the displacement perpendicular to the wire and z is the coordinate along the wire direction. $\vec{F}_e$ and $\vec{F}_g$ are the electrostatic and gravitational forces acting on the wire, respectively. Thanks to the linearity of the equation we can separate the gravitational and electrostatic parts and treat them independently.

The gravitational sag is thus governed by

$$T \cdot \frac{d^2\vec{\delta_g}}{dz^2} = \vec{F_g} = \rho \cdot \vec{g}, \tag{2}$$

where ρ is the linear density of the wire, g is the acceleration of gravity. The solution for this equation is

$$\vec{\delta_g}(z) = \frac{1}{2} \cdot \frac{\rho \cdot \vec{g}}{T} \cdot z\,(z - L)\,,$$

where L is the wire length (L=4.6m). The maximum sagitta is attained at $z = L/2$:

$$Y \equiv |\vec{\delta_g}(L/2)| = \frac{L^2}{8} \cdot \left(\frac{\rho \cdot g}{T}\right). \tag{3}$$

The calculation of the gravitational sag thus requires the measurements of the linear density and the tension. The formula recommends low density materials as long as the maximum applicable tension is the same. Notice also the quadratic dependence on the wire length, implying a potential problem with a drift chamber with long wires.

The equation for the electrostatic sag is, on the other hand, given by

$$T \cdot \frac{d^2\vec{\delta_e}}{dz^2} = \vec{F_e} = q\vec{E}, \tag{4}$$

where q and $\vec{E}$ are, respectively, the charge per unit length and the electric field at the wire which is generated by the other wires. Ignoring the z-dependence of $\vec{E}$ leads to an approximate solution:

$$\begin{pmatrix} \Delta X \\ \Delta Y \end{pmatrix} = \vec{\delta_e}(L/2) = \frac{L^2}{8} \cdot \left(\frac{q \cdot \vec{E}}{T}\right) \tag{5}$$

The formula has essentially the same structure as Eq. (3) and recommends lower charge and electric field or, in other words, lower high voltages. In addition to the wire tension, the formula requires q and $\vec{E}$ which are determined by the wire configuration (cell structure) and high voltages.

If the displacement given by Eq. (5) is so large that the field variation from that at the original position is substantial, we need to reevaluate the electric field for the new wire configuration and recalculate the sagitta. If necessary, we should repeat this procedure till the resultant displacement converges.

We have developed a software program to do this and predict the wire displacement, knowing the cell structure, wire tension, and high voltage on each wire. In order to test the prediction, we need to measure the wire tension and the wire positions accurately.

4 Wire Tension Measurement

Almost all methods of wire tension measurements are based on the same basic principle [4] and ours is no exception. We excite oscillations of a wire at its resonant frequency, and then determine the tension T by using the following relation:

$$T = 4\rho \cdot L^2 \cdot f^2, \tag{6}$$

where f is the fundamental resonant frequency. Our wire tension measurement scheme is shown in Fig.4-(a). We apply a sinusoidal current through a chamber wire, which is placed in a magnetic field (B $\simeq$30Gauss) perpendicular to the wire. The Lorentz force acting on the wire produces a mechanical oscillation. This induces an electromotive force across the wire due to Faraday's law of electromagnetic induction and modulates the current. By detecting this modulation while sweeping frequency, we can thus determine the resonant frequency.

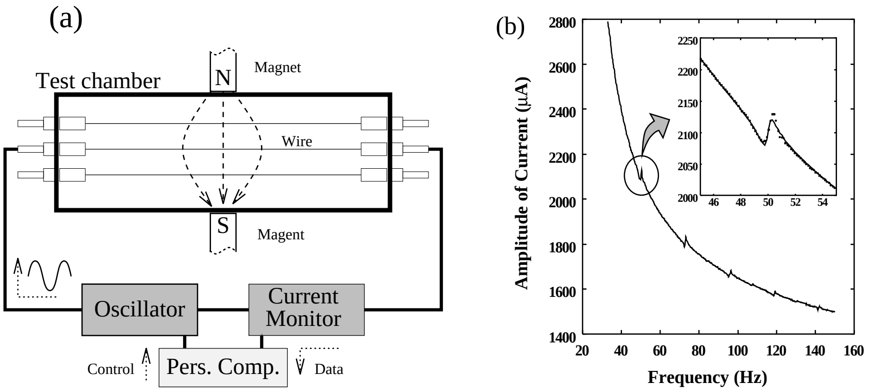

Figure 4: (a) block diagram of tension measurement system and (b) wire current as a function of frequency for a typical field wire.

A typical lineshape for an aluminum field wire is shown in Fig. 4-(b) as a function of frequency. Each tooth corresponds to a resonant frequency. The resonant frequency was determined by fitting the lineshape and the corresponding tension was calculated using Eq. (6). The results are shown in Figs. 5-(a) and -(b) for field and sense wires, respectively, as functions of the time measured from the day of wire stringing. There is still a tension drop of about 10%/year for gold-plated Al field wires unlike gold-plated W sense wires which now reach a tension plateau. Although this poses a potential problem and requires a better wire material, we are not going into details of this problem anymore in this paper. Instead, we are going to concentrate on the measurements and predictions of wire displacements, assuming the wire tensions are known somehow.

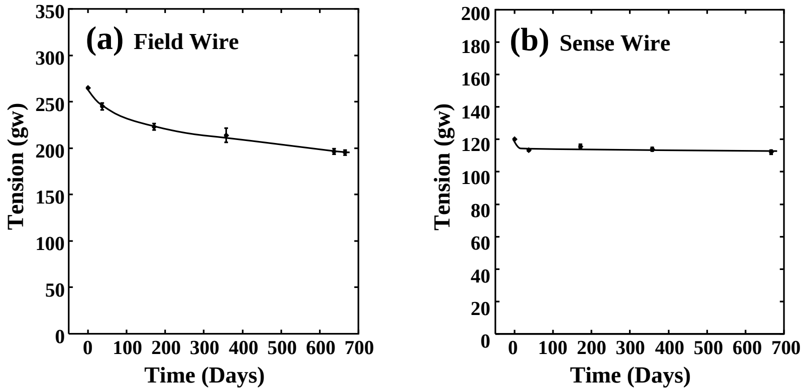

Figure 5: Tension versus time for (a) field and (b) sense wires

5 Gravitational and Electrostatic Sag Measurements

5.1 Wire Position Measurement System

As seen in Fig. 1, we used two CCD cameras, one for horizontal and the other for vertical position measurements. Each of these two cameras has an area of sight of 1 mm $\times$ 1 mm and a focal depth of $\simeq$ 1 mm, which is about 1 m away from the front face of the camera. Since the area of sight and the focal depth are so small, getting a target wire in sight is not easy. In order to help us find a wire to be measured, a laser beam spotter with a spot size of 2 mm diameter is attached to each camera body so as to illuminate the focal point.

The cameras are then mounted on precision movers and their positions are computer-controlled with a step size of 0.4 μm/pulse and are monitored by linear scales of 5 μm resolution. When the cameras are moved over a long distance, however, their tilt angle variations might introduce substantial error in absolute coordinate measurements. We have calibrated the variation of the tilt angle using an auto-collimeter and achieved an overall accuracy of $\simeq$ 10 μm.

Typical field and sense wire images from the CCD cameras are shown in Figs.6-(a) and -(b), demonstrating the resolution of our system.

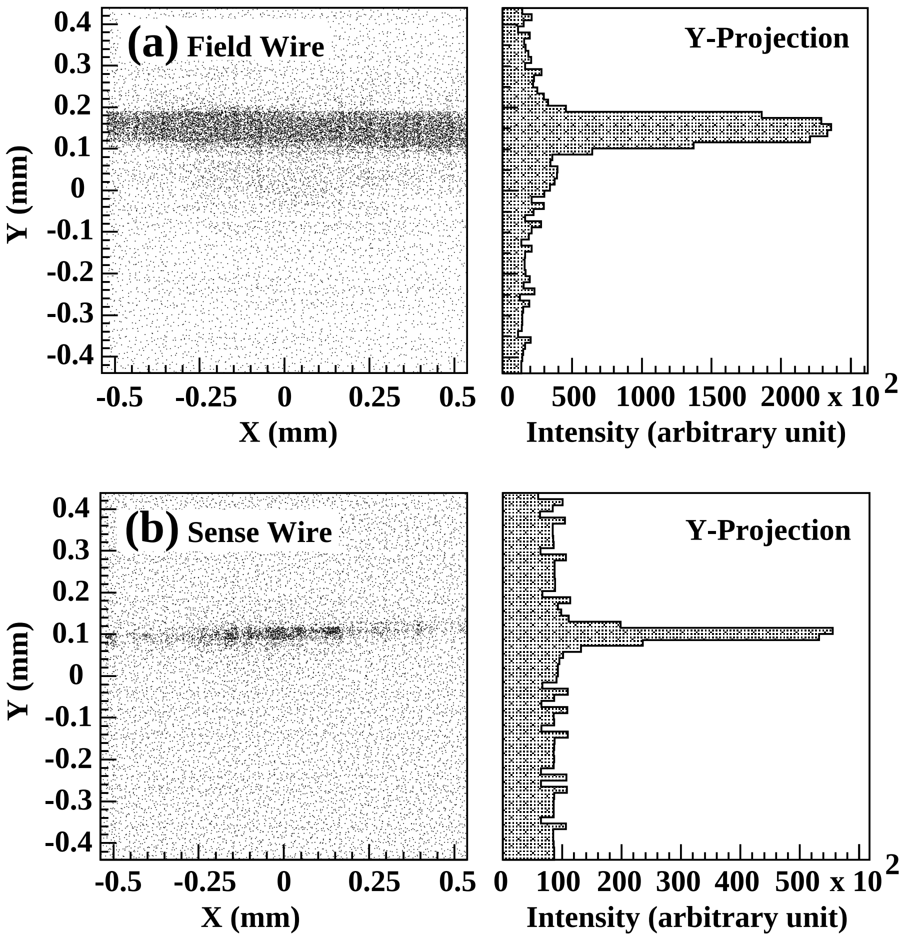

Figure 6: Typical CCD images for (a) a 125 μm field wire and (b) a 30 μm sense wire.

5.2 Gravitational Sag

Fig. 7 illustrates our measurement scheme of the gravitational sag of a wire. The measurement goes as follows. Using the vertical camera, we first put fiducial marks on the chamber windows in such a way that the line connecting them passes through the wire in question (configuration 1 in Fig. 7). Then we rotate the test chamber by 90° and determine the wire deflection due to gravitational sag by measuring the wire position relative to the line connecting the fiducial marks, using the horizontal camera (config.2 in Fig. 7).

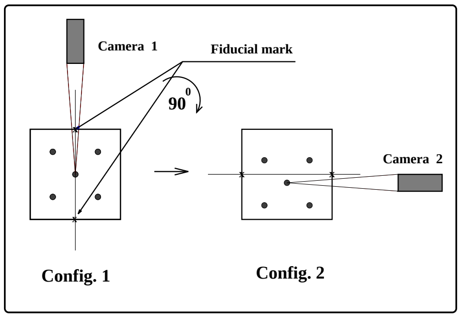

Figure 7: Principle of gravitational sag measurements

We measured the gravitational sags 1.5 years after the wire stringing and the results of the

Table 1: Results of the gravitational sag measurements and calculations

Wire name	Y(meas) (μm)	Y(calc) (μm)
S1	362	304
S2	334	312
S4	353	320
S5	363	310
G1	603	518
G2	607	562
G3	588	561
G5	621	560
G6	613	562
GR1	639	540
GR2	635	552
GR3	612	546
GR4	597	531
GL1	538	552
GL2	521	555
GL3	587	563
GL4	704	552
GL5	567	564

measurements are given in table 1. The average gravitational sags for field and sense wires were 600μm and 353μm, respectively. The results of the gravitational sag measurements and calculations using Eq. (3) are compared in table 1, showing good agreement.

5.3 Electrostatic Sag

Our measurement scheme of electrostatic sag is sketched in Fig. 8. We first get a wire in sight on both the horizontal and vertical cameras with high voltages off. Then we measure the horizontal (ΔX) and vertical (ΔY) displacements in the camera screens after turning on the high voltages. Notice that the camera stays at rest during the measurement and the measurement accuracy is determined completely by the wire image resolutions on the screens (there is no tilt angle effect here). The overall accuracy for the electric sag measurement was estimated to be 5 μm. The wire stability in the electrostatic field has been checked by turning on and off the high voltages several times. We found no instability, meaning that the wires always return to the same positions of equilibrium.

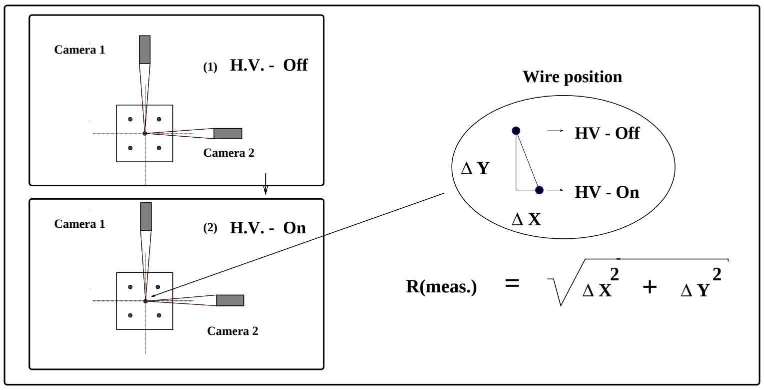

Figure 8: Schematic view of the electrostatic sag measurements.

The results of our electrostatic sag measurements are summarized in table 2 for sense wires and surrounding Al wires together with predictions. More detailed comparison will be made in the following section.

6 Discussions

Figs.9 and 10 illustrate the wire deflections in our 4.6 m test chamber due to gravitational and electrostatic forces. In the figures an *original position* ($\bigtriangledown$) is the initial position of a wire at the end plates. On the other hand, denoted as *gravitational sag* ($\Box$) and *electric sag* ($\star$) are the measured positions of the wire under the gravitational force *before* and *after* applying high voltages, respectively. Called first iteration ($\circ$) is the calculated value of the wire deflection in the electrostatic field when other wires are at the positions after the gravitational sags, which were calculated by Eq. (5). The input parameters for the second iteration ($\bullet$) are the new wire positions from iteration 1.

In Fig.9 we compare the measurements and predictions for a few field wires which are on the left and right sides of the sense wire plane. There is a good agreement not only in the magnitude of deflection but also in its direction for each one of these field wires. It is clear that the prediction from the second iteration is better.

Results of the predictions and measurements for sense wires $S1$ and $S2$ are shown in Fig.10. There is a noticeable left-right asymmetry in the measurements with respect to the original sense wire plane, which could not be reproduced by the calculation. Probably the source of such an asymmetry can be attributed to the influence of the other cells which might have some asymmetry in wire tensions, since they were strung over a finite period of time. In any case, it is now very important to ask whether these discrepancies between the measurements and the predictions are negligible or not in terms of the required spatial resolution.

In order to answer this question, we need to calculate x-t relations, since we can-

Table 2: Results of the electrostatic sag measurements and predictions

	Measurement			Calculation					
				1-st iteration			2-nd iteration		
Wire name	ΔX (μm)	ΔY (μm)	R (μm)	ΔX (μm)	ΔY (μm)	R (μm)	ΔX (μm)	ΔY (μm)	R (μm)
S1	-117	49	128	1	-1	1	3	50	50
S2	61	111	127	2	85	85	0	160	160
S3	36	96	102	-1	76	76	1	147	147
S4	-10	80	81	-1	66	66	-4	132	132
S5	-110	37	116	0	43	43	0	80	80
GL1	593	-43	594	536	-10	536	596	-13	596
GL2	552	-18	552	519	-12	519	586	-16	586
GL3	556	-26	557	511	-11	511	567	-15	567
GL4	546	-33	547	521	-9	521	579	-14	580
GL5	561	-36	562	508	-6	508	563	-9	563
GL6	522	18	523	494	1	494	543	-0.3	543
GR1	-558	-1	558	-546	-11	546	-608	-14	608
GR2	-562	-36	563	-517	-12	517	-583	-16	583
GR3	-564	-21	565	-491	-10	491	-542	-13	542
GR4	-542	-23	543	-505	-9	505	-559	-12	559
GR5	-531	-10	531	-505	-6	505	-559	-9	559
GR6	-515	-14	515	-483	1	483	-529	0.2	529
F1UL	127	-14	128	54	-10	25	85	-55	101
F1UR	-146	-51	154	-27	-23	36	-84	-54	100
F1DL	113	76	136	25	92	25	83	53	98
F1DR	-129	91	158	-30	25	39	-83	53	98

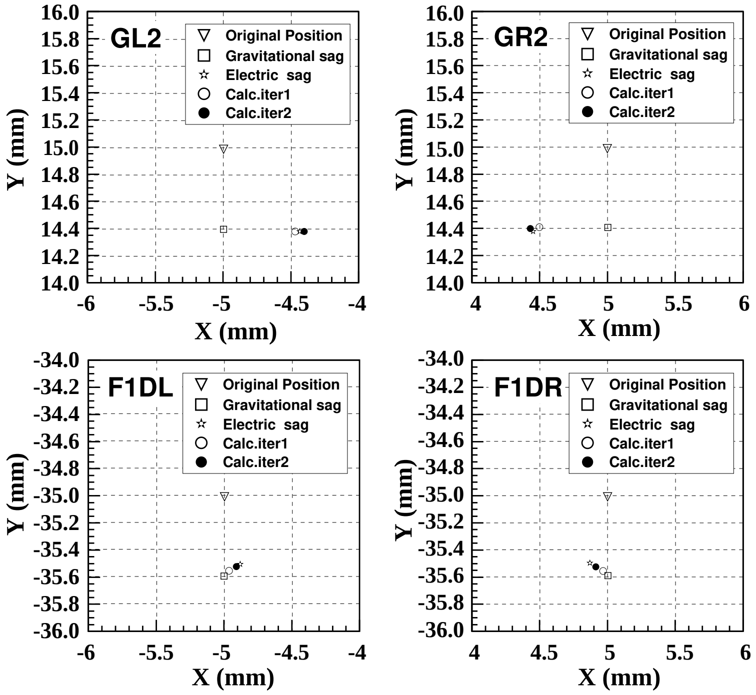

Figure 9: Measured positions of some representative field wires at the endplates ($\bigtriangledown$), with gravitational sags ($\Box$) before and ($\star$) after electrostatic sags, compared with calculations: iterations 1($\circ$) and 2 ($\bullet$).

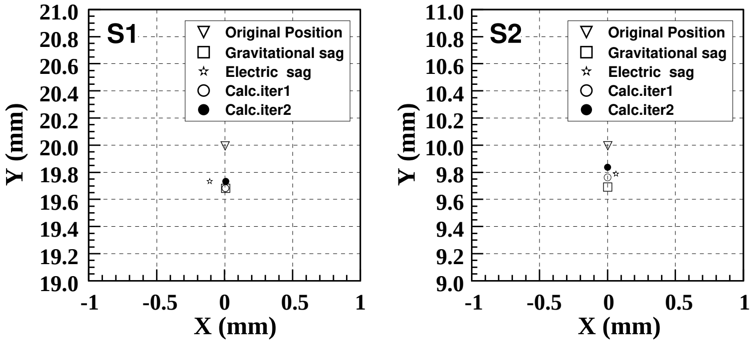

Figure 10: Same as Fig. 9 for the worst ($S1$) and a typical ($S2$) sense wires.

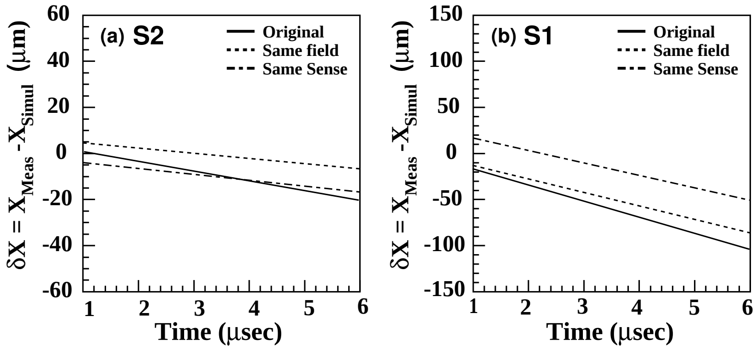

Figure 11: Difference in x between the measurement and the calculation (solid lines) for the same drift time t for (a) a typical $S2$ and (b) the worst $S1$ sense wire. The dashed lines correspond to the case in which the measured positions of field wires (near sense wires) are used in the calculation. The dot-dashed lines are the results when the measured positions of sense wires are used in the calculation.

not simply translate these discrepancies in the positions to the errors in the coordinate measurements because of the region-to-region variation of the drift velocity. We thus calculated the x-t relations with GARFIELD for measured and predicted wire positions after the gravitational and electrostatic sags.

Fig.11 shows the difference in x between the measurements and the calculations (solid lines) at the same drift time t for sense wires $S1$ and $S2$. The dashed lines correspond to the case in which the measured positions of field wires are used in the calculation. The dashed-dotted lines are the results when the measured positions of the sense wires are used instead. The error in the coordinate measurement is thus estimated to be better than 80 μm per wire even in the worst case.

7 Conclusions

We have developed a wire position measurement system. Using this we measured the gravitational and electrostatic sags. The average gravitational sags for field and sense wires are 600μm and 353μm, which are in good agreement with predictions 553μm and 312μm, respectively.

We have also developed a software program to calculate wire displacements in electrostatic fields, knowing the cell structure, wire tension, and high voltage on each wire. There is a good agreement with measurements for field wires surrounding sense wires. In the case of sense wires, there is some left-right asymmetry in measurements, which could not be reproduced by the calculations based on a single cell configuration. This is probably because some possible tension variation in the other cells destroyed the apparent symmetry of the chamber. The effect of the asymmetry on the coordinate measurements was estimated with GARFIELD and was found to be less than 80 μm at worst, demonstrating the feasibility of an initial wire alignment which is accurate enough to make later more precise software alignments practicable.

Acknowledgments

The authors would like to thank all the members of the JLC physics working group for useful discussions. In particular, Y. Fujii and T. Matsui deserve special mention. The authors are very much indebted to T. Naito for suggesting us the use of a CCD camera for wire position measurements and to M. Iwai for designing the chamber mechanical structure and the precision mover of the CCD camera system. They are also grateful to other members of the KEK technical staff including K. Hayashi, T. Koriki, and Y. Yamaoka.

References

[1] JLC group, KEK Report 92-16, December,1992.

[2] Even in the presence of some wire-to-wire variation of the gravitational sags, the local field configuration at some given z position can still be calculated, if we use the local wire positions instead of the nominal ones at the endplates.

[3] Veen Hove, A Drift Chamber simulation program GARFIELD, 1994.

[4] T.Regan, Nucl. Inst. and Meth. A219 (1984) 100; S.Bhadra et al., Nucl. Instr. and Meth. A269 (1988) 33; E.R.Mueller, Nucl.Instr. and Meth. A281 (1989) 652.